BBA - Molecular Cell Research 1872 (2025) 119998

Contents lists available at ScienceDirect

BBA - Molecular Cell Research

journal homepage: www.elsevier.com/locate/bbamcr

Impact of PARL-mediated mitochondrial protease activity on calcium regulation

Donato D'Angelo [a,1], Aya Al Saidi [a,1], Giorgia Ghirardo [a,1], Denis Vecellio Reane [a], Nicola Gasparini [a], Rosario Rizzuto [a,b,*], Anna Raffaello [a,c,*]

[a] Department of Biomedical Sciences, University of Padua, Padua, Italy
[b] National Center on Gene Therapy and RNA-Based Drugs, 35131 Padua, Italy
[c] Myology Center (CIR-Myo), University of Padua, 35131 Padua, Italy

ARTICLE INFO

Keywords:
Calcium signaling
Rhomboid protease
Mitochondrial intermembrane proteolysis
PARL
Mitochondria
Mitochondrial calcium uniporter

ABSTRACT

The presenilin-associated rhomboid-like protein (PARL) is a mitochondrial inner membrane serine protease that is a key regulator of several cellular processes, including apoptosis, metabolism, inflammation and stress responses. While recent studies suggest that PARL may play a role in mitochondrial calcium homeostasis, the underlying mechanisms remain poorly understood. In this study, we investigated the effects of PARL modulation on mitochondrial and cytosolic calcium dynamics, as well as mitochondrial membrane potential. Our results show that altering PARL protein levels, through both overexpression and silencing, significantly affects mitochondrial calcium uptake, without influencing cytosolic calcium transients or mitochondrial membrane potential. Despite the observed changes in mitochondrial calcium dynamics, PARL does not interact with the mitochondrial calcium uniporter complex (mtCU) regulators MICU1 and MICU2, which are critical for regulating mitochondrial calcium influx. However, we observed alterations in the protein levels of MICU1 and MICU2, either in their monomeric or dimeric forms, suggesting that PARL may influence these mtCU components indirectly. Interestingly, the pore-forming subunit MCU, and the structural subunit EMRE, essential for the assembly of the mtCU, were unaffected by PARL modulation. These findings suggest that the role of PARL in modulating mitochondrial calcium homeostasis may involve indirect mechanisms, potentially involving other regulatory pathways. Overall, our study provides novel insights into the functional role of PARL in mitochondrial calcium regulation, offering potential avenues for further investigation into its broader cellular functions.

1. Introduction

Mitochondria are highly dynamic organelles that constantly adapt to cellular conditions and exposure to stressors, such as oxidative damage [1,2]. Effective mitochondrial quality control plays a crucial role in preserving mitochondrial function and plasticity [3]. Mitochondrial proteases play a central role in this process by ensuring proper protein processing and degradation of dysfunctional or damaged proteins, thereby maintaining mitochondrial integrity [4,5]. The mitochondrial protease PARL (PINK1/PGAM5 associated rhomboid-like protease) is a member of the rhomboid family of serine proteases [6–8], localized in a proteolytic hub in the inner mitochondrial membrane (IMM), the SPY complex. It comprises the i-AAA protease YME1 like 1 ATPase (YME1L), and stomatin-like 2 protein (SLP2) acting as a scaffold for the two proteases [9]. PARL has received particular attention due to its implication in several pathological conditions [7,8]. In the context of metabolic diseases, studies have shown that PARL gene expression is significantly reduced in diabetic rodents [10]. Further evidence from human studies indicates a reduction in both PARL gene and protein expression in patients with type 2 diabetes [11], with the L262V polymorphism linked to elevated plasma insulin levels [12,13]. Moreover, the downregulation of this protease in skeletal muscle has been shown to impair insulin signaling in mice [11]. In the context of neurodegenerative disorders, the S77N mutation in the PARL gene has been identified in two patients with Parkinson's disease, suggesting a potential pathogenetic role [14]. However, the exact contribution of PARL to these diseases remains unresolved.

The PTEN-induced putative kinase protein 1 (PINK1) is the first and

* Corresponding authors at: Department of Biomedical Sciences, University of Padua, Padua, Italy.
E-mail addresses: rosario.rizzuto@unipd.it (R. Rizzuto), anna.raffaello@unipd.it (A. Raffaello).
[1] Equal contribution

https://doi.org/10.1016/j.bbamcr.2025.119998
Received 18 February 2025; Received in revised form 28 May 2025; Accepted 5 June 2025
Available online 6 June 2025
0167-4889/© 2025 The Authors. Published by Elsevier B.V. This is an open access article under the CC BY license (http://creativecommons.org/licenses/by/4.0/).

most extensively studied substrate of PARL [15,16]. In healthy mitochondria, PARL cleavage of PINK1 allows its release from mitochondria to the cytosol, where it is subsequently degraded by the ubiquitin-proteasome system [17,18]. However, in depolarized mitochondria, PINK1 accumulates on the outer mitochondrial membrane (OMM), preventing its cleavage by PARL [17,19]. Exposed PINK1 on OMM recruits the E3 ubiquitin ligase Parkin, which triggers mitophagy [20]. In response to mitochondrial stress, such as membrane depolarization, PARL cleaves the phosphoglycerate mutase member 5 (PGAM5), leading to its translocation to the cytosol, promoting a pro-apoptotic signaling cascade [21]. Furthermore, PARL has been shown to play a pro-apoptotic role through its cleavage of Smac/DIABLO [22,23]. PARL-mediated cleavage releases a portion of Smac into the cytosol, which is required for its apoptotic function [23]. This critical role of PARL in regulating the localization of various substrate proteins has also been highlighted by its cleavage during mitochondrial import of the STAR-related lipid transfer domain protein 7 (STARD7), partitioning it between the cytosol and the mitochondrial intermembrane space (IMS), preserving mitochondrial membrane homeostasis [24].

Deletion of PARL in the mouse brain results in the loss of tetratricopeptide 19 (TTC19), a regulator of complex III activity, resulting in neuronal necrosis and a Leigh-like syndrome [25]. Remarkably, this model also exhibits alterations in mitochondrial calcium (Ca^{2+}) homeostasis [25]. A putative role of PARL in regulating mitochondrial Ca^{2+} homeostasis is also supported by a recent proteomic study showing a direct interaction between PARL and the essential MCU regulator (EMRE), a structural subunit essential for the assembly of the mitochondrial Ca^{2+} uniporter complex (mtCU) [26–28]. Moreover, the most recently identified substrate of PARL, the Caseinolytic peptidase B protein homolog (CLPB), a disaggregase localized in the IMS, has been shown to regulate the solubility of mitochondrial calcium uptake 2 (MICU2), a key regulatory subunit of the mtCU [29–31].

In this study, we investigate the impact of PARL modulation on mitochondrial Ca^{2+} homeostasis. Our findings show that both upregulation and downregulation of PARL protein levels lead to an increase in mitochondrial Ca^{2+} uptake, without altering cytosolic Ca^{2+} transients or mitochondrial membrane potential. Furthermore, we observed changes in the level of MICUs protein, though no direct interaction with PARL was identified. Based on these results, we conclude that PARL influences mitochondrial Ca^{2+} homeostasis, likely through indirect mechanisms.

2. Results

2.1. Both overexpression and silencing of PARL lead to increased mitochondrial Ca^{2+} uptake

Since a recent proteomic study showed that PARL directly interacts with the essential MCU regulator EMRE, we asked whether this protein could play a role in the modulation of mitochondrial Ca^{2+} homeostasis. We started our analysis by assessing the impact of PARL on mitochondrial Ca^{2+} uptake by overexpressing it in HeLa cells for 48 h. To measure mitochondrial Ca^{2+} concentration ($[Ca^{2+}]_{mt}$), we transfected HeLa cells with the mitochondrially targeted aequorin probe and upon maximal histamine stimulation, $[Ca^{2+}]_{mt}$ was significantly increased in cells overexpressing PARL compared to control cells (Fig. 1A, B). To determine whether this increase in mitochondrial Ca^{2+} uptake was caused by alterations in cytosolic Ca^{2+} concentration ($[Ca^{2+}]_{cyt}$), we performed a similar experiment using the cytosolic aequorin probe. Quantification of the peak $[Ca^{2+}]_{cyt}$ levels upon maximal histamine stimulation showed no significant difference between PARL-overexpressing and control cells (Fig. 1C, D). No changes were observed in normalized $[Ca^{2+}]_{mt}$ and $[Ca^{2+}]_{cyt}$ influx (Fig. S1A, B), as well as normalized $[Ca^{2+}]_{mt}$ and $[Ca^{2+}]_{cyt}$ efflux (Fig. S1C, D) in both control and PARL overexpressed cells.

We also investigated the effect of PARL silencing on mitochondrial and cytosolic Ca^{2+} uptake. HeLa cells were transfected with esiRNA

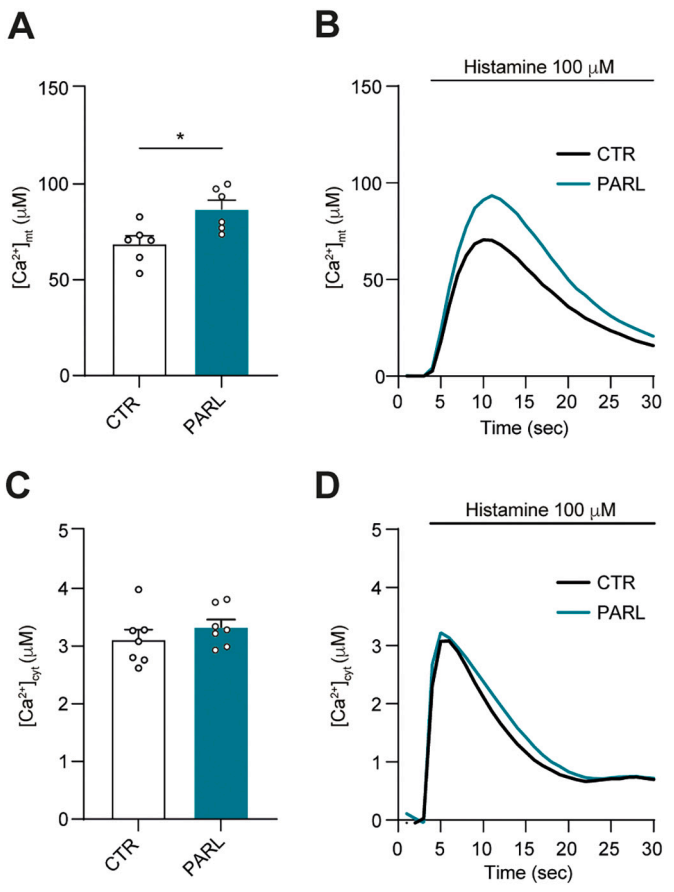

Fig. 1. PARL overexpression increases mitochondrial Ca^{2+} uptake without affecting cytosolic Ca^{2+} transients. (A) $[Ca^{2+}]_{mt}$ in intact HeLa cells overexpressing PARL for 48 h together with mitochondrially targeted aequorin, challenged with maximal histamine stimulation. The bar diagram represents the mean peak ± SEM. $n = 6$ for each condition. * $p \leq 0.05$ compared to the control (CTR). (B) Representative traces of the experiment performed shown in A. (C) $[Ca^{2+}]_{cyt}$ in intact HeLa cells overexpressing PARL for 48 h together with cytosolic aequorin, challenged with maximal histamine stimulation. The bar diagram represents the mean peak ± SEM. $n = 7$ for each condition. (D) Representative traces of the experiment shown in C.

targeting PARL for 72 h, and $[Ca^{2+}]_{mt}$ was measured, similarly to what performed in the overexpression experiments. PARL silencing resulted in a significant increase in mitochondrial Ca^{2+} uptake (Fig. 2A, B). To test whether the increase in $[Ca^{2+}]_{mt}$ could be secondary to changes in cytosolic Ca^{2+} homeostasis, we transfected cells with cytosolic aequorin in either control or PARL silencing HeLa cells. In this experiment, $[Ca^{2+}]_{cyt}$ remained unchanged, with no significant difference observed between the control and PARL-silenced cells (Fig. 2C, D). Likewise, no changes were observed in the normalized influx (Fig. S2A, B) and efflux (Fig. S2C, D) of $[Ca^{2+}]_{mt}$ and $[Ca^{2+}]_{cyt}$ in both control and PARL silenced cells. Since PARL modulation only mildly increases mitochondrial Ca^{2+} uptake, we reduced the histamine concentration to 10 μM to assess whether lower stimulation would better reveal differences in MCU regulation associated with PARL modulation (Fig. S3A—D). Notably, the observed results were similar to the response at 100 μM histamine concentration, suggesting that the increase in mitochondrial Ca^{2+} uptake is not dependent on the intensity of the stimulation, but rather on the effect of PARL modulation.

Taken together, these results indicate that both overexpression and silencing of PARL enhance mitochondrial Ca^{2+} uptake without altering cytosolic Ca^{2+} homeostasis. This suggests a potential role for PARL in regulating mitochondrial Ca^{2+} homeostasis through mechanisms independent of cytosolic Ca^{2+} transients.

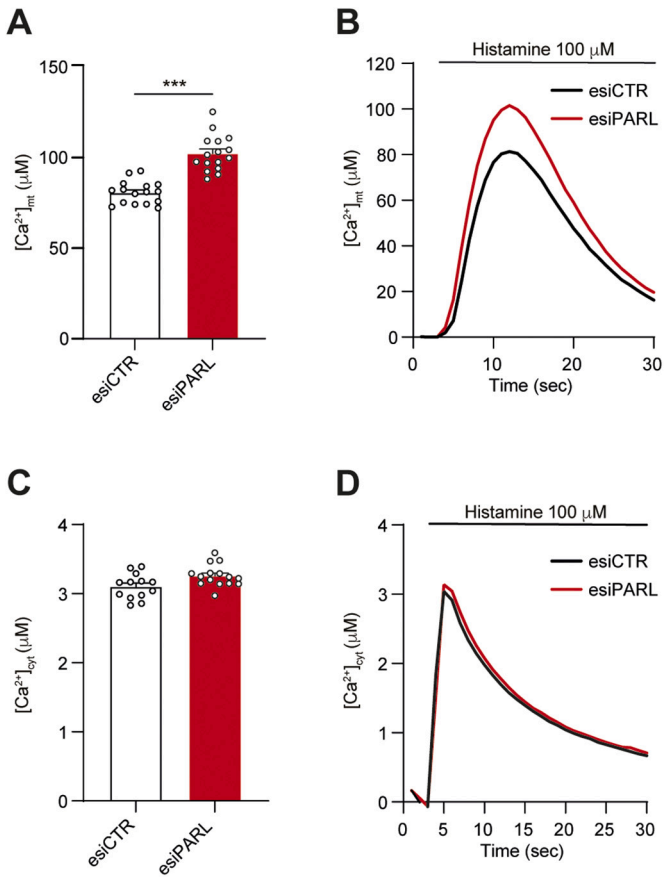

Fig. 2. PARL silencing increases mitochondrial Ca^{2+} uptake without affecting cytosolic Ca^{2+} transients. (A) $[Ca^{2+}]_{mt}$ in intact HeLa cells silencing PARL for 72 h together with the overexpression of mitochondrially targeted aequorin, challenged with maximal histamine stimulation. The bar diagram represents the mean peak ± SEM. $n = 16$ for each condition. *** $p \leq 0.001$ compared to the control (esiCTR). (B) Representative traces of A. (C) $[Ca^{2+}]_{cyt}$ in intact HeLa cells silencing PARL for 72 h together with overexpressing cytosolic aequorin, challenged with maximal histamine stimulation. The bar diagram represents the mean peak ± SEM. $n = 13$ for esiCTR, and $n = 15$ for esiPARL. (D) Representative traces of the experiment shown in C.

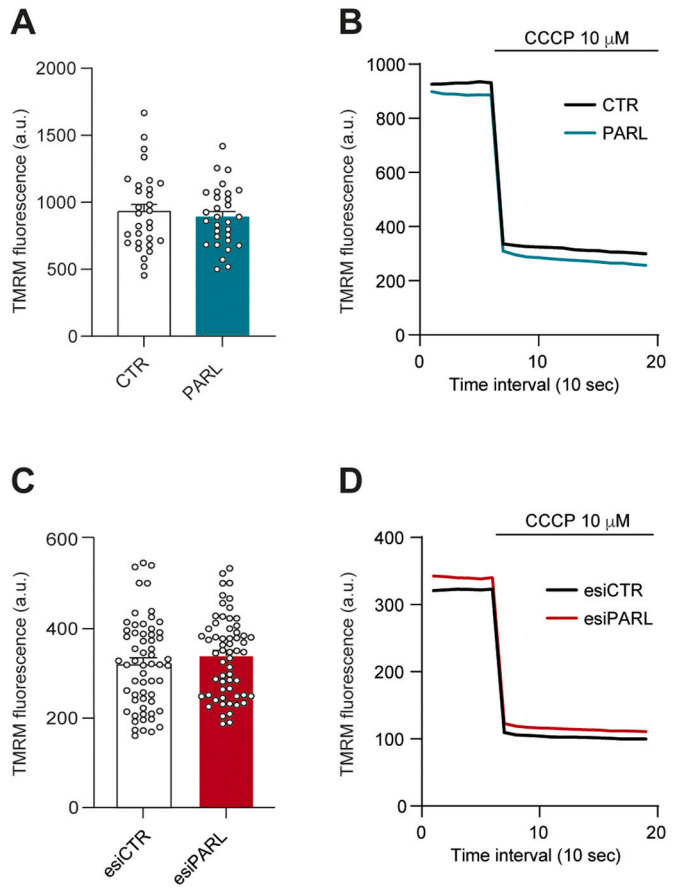

Fig. 3. PARL overexpression and silencing do not alter mitochondrial membrane potential. (A) Tetramethyl rhodamine methyl ester (TMRM) fluorescence measurements in HeLa cells overexpressing PARL for 48 h. The bar diagram represents the mean ± SEM. $n = 30$ for each condition. (B) Representative traces of the experiment shown in A. Where indicated 10 μM CCCP were added. a.u., arbitrary units. (C) TMRM fluorescence measurements in HeLa cells silencing PARL for 72 h. The bar diagram represents the mean ± SEM. $n = 60$ for each condition. (D) Representative traces of the experiment shown in C. Where indicated 10μM CCCP were added. a.u., arbitrary units.

2.2. PARL modulation does not alter mitochondrial membrane potential (ΔΨm)

To investigate whether the increase in mitochondrial Ca^{2+} uptake upon PARL overexpression or silencing was secondary to changes in the mitochondrial membrane potential (ΔΨm), we measured ΔΨm using the potentiometric dye tetramethyl rhodamine methyl ester (TMRM). Both PARL overexpression (Fig. 3A, B) and PARL silencing (Fig. 3C, D) did not alter the ΔΨm, indicating that the ΔΨm is not the cause of the observed changes at the mitochondrial Ca^{2+} levels.

2.3. PARL overexpression decreases MICU1 protein level, while PARL silencing does not affect the mtCU components protein level

To investigate whether the observed alterations in mitochondrial Ca^{2+} dynamics are caused by changes in the abundance of the mtCU components, we performed immunoblotting analysis in HeLa cells overexpressing and silencing PARL. We first assessed whether PARL overexpression modulates the protein expression of mtCU subunits. The overexpression of PARL was confirmed by the increased levels of PARL protein (Fig. 4A, B). Notably, overexpression of PARL resulted in a significant reduction in MICU1 protein levels (Fig. 4A, B), whereas MICU2, EMRE and MCU expression remained unchanged (Fig. 4A, B). Secondly, we assessed the effect of transient silencing of PARL on the mtCU components. As expected, a significant reduction in PARL protein levels was confirmed after 72 h upon silencing (Fig. 4C, D). However, the expression levels of the mtCU components were unaffected by PARL depletion (Fig. 4C, D). These results indicate that while the overexpression of PARL can affect mtCU protein abundance, its silencing does not influence it.

2.4. PARL overexpression does not change MICUs dimers, while PARL silencing decreases MICU1-MICU2 heterodimers

MICU1 and MICU2 bound the mtCU in dimeric form, composed either by MICU1 homodimers or MICU1-MICU2 heterodimers, modulating the sigmoidal response of mitochondrial Ca^{2+} uptake [31]. Since we observed changes in the MICU1 monomeric form upon PARL overexpression, we performed immunoblotting experiments in non-reducing conditions to analyze the levels of the MICUs dimers. MICU1 can form homodimers with itself, with an approximative molecular weight of 100 kDa, or heterodimers with MICU2, with the approximative molecular weight of 95 kDa [31]. Therefore, MICU1 antibody detects both forms, while MICU2 antibody specifically detects the MICU1-MICU2 heterodimeric form. Importantly, in HeLa cells, the MICU1-MICU2 heterodimers is the predominant form [31]. Despite the observed reduction in MICU1 monomer levels upon PARL overexpression, MICU1–MICU2

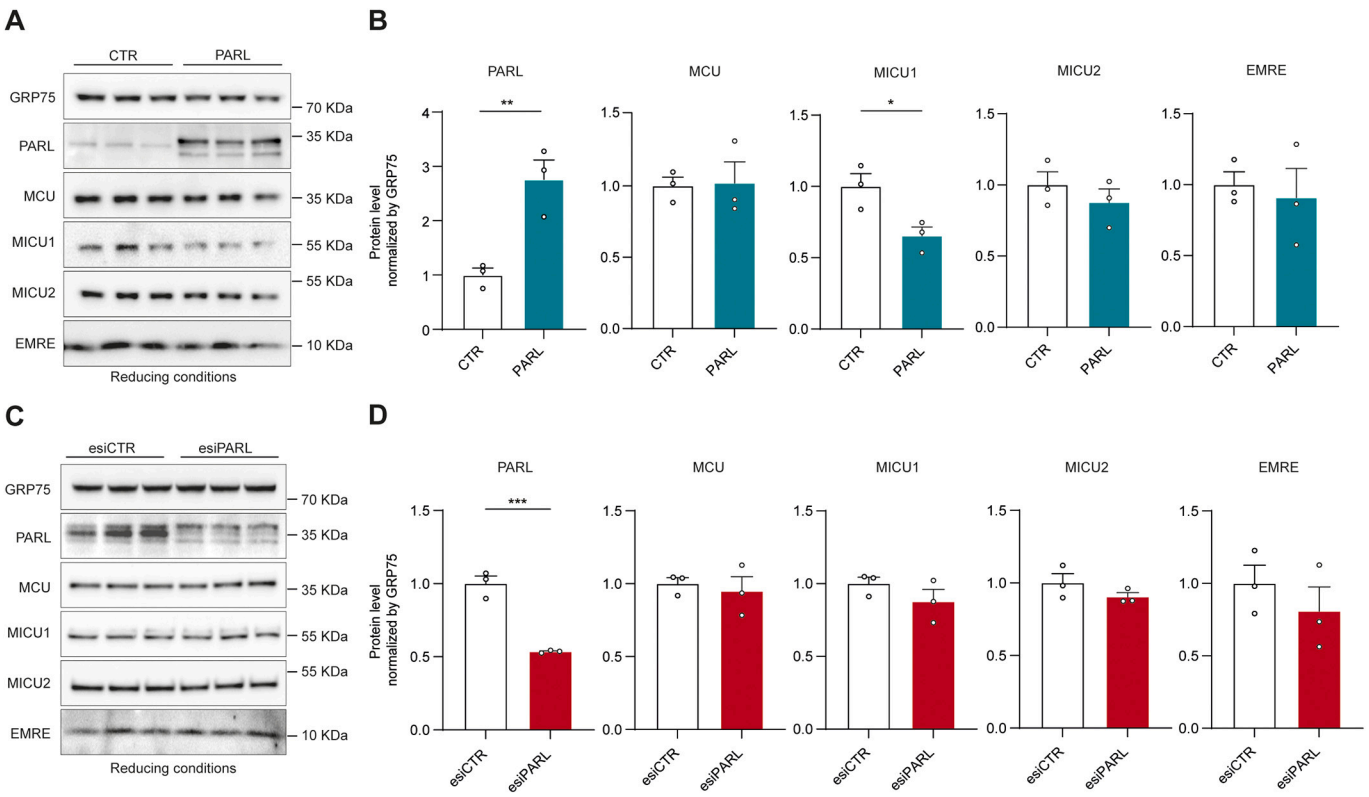

Fig. 4. PARL overexpression decreases MICU1 protein levels while its silencing does not affect mtCU expression. (A) Representative western blot of the mtCU components and PARL obtained from total protein extract of control (CTR) and PARL overexpressing HeLa cells harvested 48 h after transfection. $n = 3$. (B) Quantification of the western blot shown in A. (C) Representative western blot of the mtCU components and PARL obtained from total protein extract of esiCTR and esiPARL silenced HeLa cells harvested 72 h after transfection. n = 3. (D) Quantification of the western blot shown in C.
In all panels, protein levels were normalized by GRP75 levels. The bar diagrams represent the mean ± SEM. n = 3 for each condition. * $p \leq 0.05$, ** $p \leq 0.01$, and *** $p \leq 0.001$ compared to the control (CTR or esiCTR).

heterodimer levels remained unchanged, although a non-significant trend toward reduction was observed (Fig. 5A, B). Interestingly, PARL silencing led to a mild but significant reduction in MICU1-MICU2 dimer expression (Fig. 5C, D). Overall, these findings indicate that the loss of PARL can lead to changes in the MICUs dimers.

2.5. PARL does not interact with MICU1 and MICU2

Given the observed changes in MICUs protein level upon PARL modulation, we investigated whether these regulatory components of the mtCU could potentially interact with PARL. To assess this, we performed co-immunoprecipitation (Co-IP) experiments in HeLa cells transfected with FLAG-tagged PARL together with HA-tagged MICU1 and MICU2. Immunoprecipitation using an α-Flag agarose-conjugated antibody successfully enriched Flag-PARL, as confirmed by immunoblotting with an anti-Flag antibody (Fig. 6A). Subsequent probing with an anti-HA antibody revealed no detectable interaction between PARL and MICU1 or MICU2, suggesting that PARL does not associate with these MCU regulatory subunits under the tested conditions (Fig. 6A).

Previous reports indicate that PARL forms a macromolecular complex in the IMM together with the i-AAA protease YME1L and the scaffolding proteins SLP2 [9]. We confirmed the interaction between PARL and YME1L by Co-IP experiment followed by immunoblotting with anti-YME1L and anti-PARL antibodies (Fig. 6B). Since it is known that MICU1 is a substrate of YME1L [33], and we found that PARL affects mitochondrial Ca^{2+} uptake, this interaction suggests a potential functional relationship between PARL and YME1L, which may be relevant for mitochondrial Ca^{2+} homeostasis.

2.6. PARL silencing does not alter the protein levels of AFG3L2, CLPB and TMBIM5, while the enhanced mitochondrial Ca^{2+} uptake observed with PARL overexpression occurs via interconnected mechanisms with YME1L

To further explore the impact of PARL modulation on mitochondrial Ca^{2+} homeostasis, we examined alternative regulators of mitochondrial Ca^{2+} handling, including TMBIM5 [34,35], AFG3L2 [36] and CLPB [29,37]. Immunoblot analysis in control HeLa cells and cells silencing PARL confirmed efficient knockdown, as indicated by reduced PARL protein levels (Fig. 7A, B). However, the protein levels of AFG3L2, TMBIM5, and CLPB remained unchanged, suggesting that their expression is not influenced by PARL downregulation (Fig. 7A, B).

Next, to determine whether the increase in mitochondrial Ca^{2+} uptake upon PARL overexpression is mediated by the i-AAA protease YME1L, a known PARL interactor [9], we performed mitochondrial Ca^{2+} measurements in HeLa cells overexpressing PARL alone or in combination with either YME1L overexpression or silencing (Fig. 7C-F). PARL overexpression significantly enhanced mitochondrial Ca^{2+} uptake as also observed for both overexpression and silencing of YME1L (Fig. 7C, D). However, the co-modulation of YME1L (either through overexpression or silencing) and PARL did not produce an additive effect (Fig. 7C-F).

3. Discussion

PARL is an IMM rhomboid protease that plays a central role in various mitochondrial functions, influencing key physiological processes such as mitochondrial dynamics, protein quality control, and apoptosis and pathological states such as neurodegenerative disease and

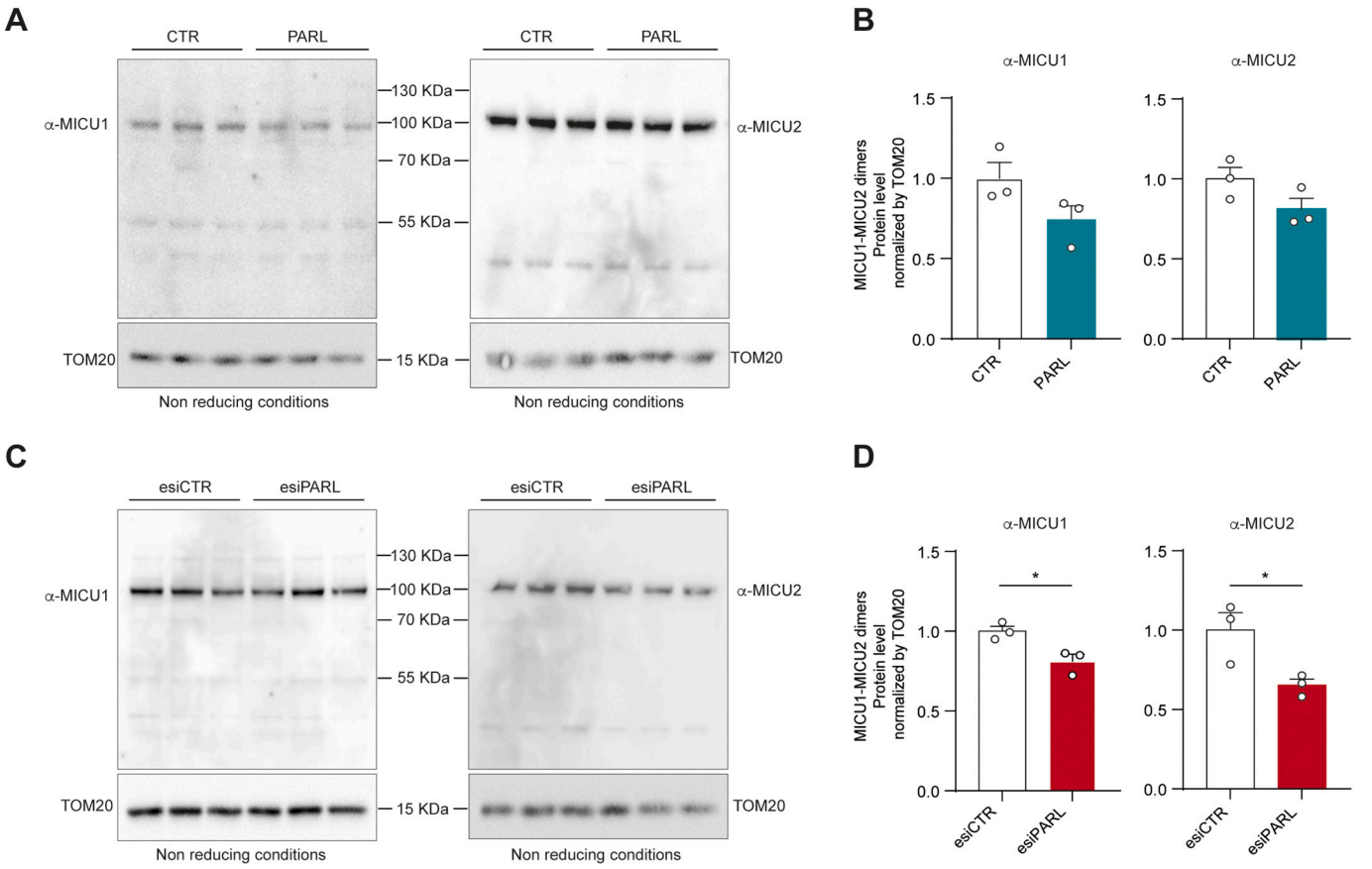

Fig. 5. PARL overexpression does not alter the MICUs dimers, while PARL silencing leads to a decrease in the MICU1-MICU2 dimers. (A) Representative western blot of MICU1-MICU2 dimers performed in non-reducing conditions from total protein extract of control (CTR) and overexpressing PARL for 48 h. TOM20 was used as a loading control. (B) Quantification of the western blot shown in A. The bar diagrams represent the mean ± SEM. n = 3 for each condition. (C) Representative western blot of MICU1-MICU2 dimers performed in non-reducing conditions from total protein extract of esiCTR and esiPARL silenced for 72 h. TOM20 was used as a loading control. (D) Quantification of the western blot shown in C. The bar diagrams represent the mean ± SEM. n = 3 for each condition. * $p \leq 0.05$.

type 2 diabetes [7]. Recent studies have suggested that PARL might also be involved in the regulation of mitochondrial Ca^{2+} homeostasis, though its exact role remains to be fully understood [25,26]. In this study, we provide evidence that modulation of PARL, through both overexpression and silencing, leads to significant alterations in mitochondrial Ca^{2+} uptake. Specifically, we observe that both the increase and the reduction of PARL expression in HeLa cells result in increased mitochondrial Ca^{2+} uptake, underscoring its potential involvement in the tight balance of mitochondrial Ca^{2+} regulation.

Our study reveals that PARL not only influences mitochondrial Ca^{2+} uptake but also the protein content of critical mtCU subunits. Specifically, PARL modulation results in changes to the protein levels of the MICUs, whether in their monomeric or dimeric forms. The formation of MICU1-MICU2 heterodimers is a tightly regulated event, and impairment in the dimerization process results in ungated mtCU, and increased mitochondrial Ca^{2+} uptake [38,39]. However, despite the observed changes at the protein level, our data did not reveal an interaction between PARL and either MICU1 or MICU2. While this finding suggests that PARL may not be within the same complex with MICU1 and MICU2, it does not rule out the possibility that the MICUs are substrates of PARL. It is possible that such protease-substrate interactions are transient and, therefore, difficult to capture using Co-IP, a technique typically used to detect stable complexes. Furthermore, PARL has been shown to alter its substrate preference under mitochondrial stress conditions [21]. Thus, is not possible to exclude that PARL's proteolytic activity can differentially affect the mtCU in response to specific stress signals.

An alternative hypothesis is that the effects of PARL on MICUs could occur via an indirect mechanism. In support of this, we observed that PARL associates with the i-AAA protease YME1L, which, as previously reported, is part of a larger proteolytic complex anchored to the inner mitochondrial membrane (IMM) by the scaffolding protein SLP2 [9]. This raises the possibility that PARL influences MICU levels through YME1L, either by altering its activity or through a proteolytic cascade. Mitochondrial Ca^{2+} measurements in HeLa cells overexpressing PARL in combination with either YME1L overexpression or silencing revealed no addictive effect, suggesting that PARL and YME1L modulate mitochondrial Ca^{2+} via interconnected mechanisms. Interestingly, both overexpression and silencing of YME1L increased mitochondrial Ca^{2+} uptake. This seemingly paradoxical finding can be explained by previous evidence showing that MICU1 is a substrate of YME1L [33,37], and both MICU1 overexpression and silencing can promote mitochondrial Ca^{2+} uptake [31].

Moreover, a recent study has shown that CLPB, a mitochondrial disaggregase, is a substrate of PARL [29]. PARL cleaves CLPB, enhancing its disaggregase activity, which is critical for maintaining protein solubility within the mitochondria [29]. CLPB has been shown to be essential for the solubility of the MICUs; in its absence, there is a marked increase in the insolubility of both MICU1 and MICU2 proteins [37]. This suggests that PARL might modulate MICUs through an additional indirect mechanism, where the cleavage and activation of CLPB by PARL could contribute to the proper solubility and function of MICUs. To investigate this possibility, we examined CLPB expression upon PARL silencing and observed no significant changes, indicating that CLPB is unlikely to contribute to the observed phenotype. Furthermore, both CLPB overexpression and silencing reduce mitochondrial Ca^{2+} uptake [37], supporting a CLPB-independent mechanism.

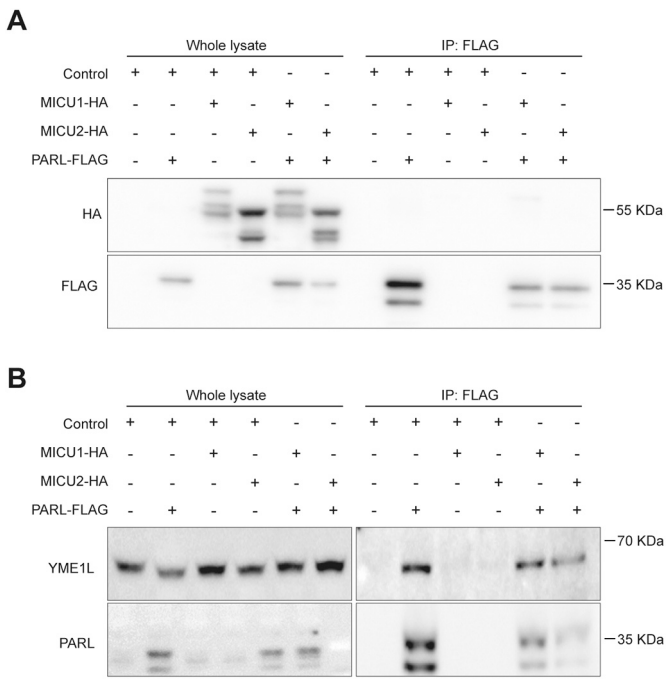

Fig. 6. PARL interacts with YME1L, but not with MICU1 and MICU2. (A) Co-immunoprecipitation experiment in HeLa cells transfected with the indicated constructs. Flag-tagged PARL was immunoprecipitated from total protein extracts with a specific α-Flag agarose-conjugated antibody. The precipitated proteins were immunoblotted with anti-Flag and anti-HA antibodies. n = 3. (B) Co-immunoprecipitation experiment as performed in A, with precipitated proteins immunoblotted with anti-PARL and anti-YME1L antibodies. $n = 2$.

Similar results were obtained when examining other regulators of mitochondrial Ca^{2+} handling, including the m-AAA protease, AFG3L2 [36], and the recently identified mitochondrial Ca^{2+} efflux mediator, TMBIM5 [34,35].

In summary, by positively or negatively modulating the expression of PARL, we have provided a characterization of its functional impact on mitochondrial Ca^{2+} homeostasis. Our results suggest a complex network of proteolytic regulation that impacts MICU solubility, function, and, consequently, mitochondrial Ca^{2+} uptake. Overall, these findings highlight the complexity of PARL's involvement in mitochondrial regulation and point to the need for further exploration into the intricated proteolytic networks that control mitochondrial Ca^{2+} dynamics.

4. Materials and methods

4.1. Cell culture and transfection

HeLa cells were cultured in Dulbecco's Modified Eagle Medium (DMEM) (Thermo Fischer Scientific, Cat #41966029), supplemented with 10 % Fetal Bovine Serum (FBS) (Thermo Fischer Scientific, Cat #10500064), 1 % penicillin (100 U/ml), and streptomycin (100 μg/ml) (Euroclone, Cat #ECB3001) at 37 °C under 5 % CO_2. The cells were transfected using a standard Ca^{2+}-phosphate method, as previously described [40]. As a control, an empty vector (pcDNA3.1) was used in the overexpression experiments, while a non-targeting siRNA or esiRNA served as the control in the silencing experiments.

4.2. siRNA and constructs

MISSION esiRNA targeting human PARL pcDNA3 (Cat #EHU115721), MISSION siRNA Universal Negative Control #2 (Cat #SIC002), and MISSION esiRNA targeting RLUC (esiCTR, Cat #EHURLUC) were purchased from Sigma-Aldrich, while the siRNA targeting YME1L was purchased from Invitrogen (Cat #HSS174400). PARL-FLAG-CT wild type was purchased from Addgene (Cat #13639).

4.3. Western blotting

HeLa cells were lysate in RIPA buffer (150 mM NaCl, 1 mM EGTA, 50 mM Tris-HCl pH = 8, 1 % Triton X-100. 0.5 % sodium deoxycholate, 0.1 % SDS), supplemented with Complete EDTA-free Protease Inhibitor cocktail (Roche, Cat #11836170001), and Phosphatases Inhibitor cocktail (Roche, Cat #4906837001). After a 30-min incubation on ice, crude extracts were centrifuged at 4 °C at 15000*g* for 10 min, to remove debris. The resulting supernatants, containing the extracted proteins, were quantified using the BCA Protein Assay Kit (Thermo Fisher Scientific, Cat #23223 and #23224). For Western blotting, 20 μg of protein extracts were mixed with NuPAGE LDS Sample Buffer (Thermo Fisher Scientific, Cat #NP0007) and 100 mM dithiothreitol (DTT) (Sigma-Aldrich, Cat #D0632), and heated at 95 °C for 5 min. Proteins were then separated by SDS-PAGE on 4–12 % Bis-Tris NuPAGE gels (Thermo Fisher Scientific, Cat #NP0321BOX) and transferred to a nitrocellulose membrane (Thermo Fisher Scientific, Cat #LC2000) via semi-dry electrophoretic transfer (Bio-Rad Cat #1704150). Membranes were blocked for 1 h at room temperature with either 5 % non-fat dry milk in TBS-T (50 mM Tris-HCl, 150 mM NaCl, 0.1 % Tween) or 5 % bovine serum albumin (BSA) (Sigma-Aldrich, Cat #A7030), depending on the primary antibody used. After primary antibody incubation overnight at 4 °C, membranes were washed in TBS-T and incubated with secondary HRP-conjugated antibodies (Bio-Rad) for 1 h at room temperature. Chemiluminescent detection was performed using SuperSignal Pico (Thermo Fisher Scientific, Cat #34580). The primary antibodies used were: anti-PARL (Novus Biologicals, Cat #NBP144262), anti-MCU (Cell Signaling Technology, Cat #14997S), anti-MICU1 (Sigma-Aldrich, Cat #HPA037480), anti-MICU2 (Sigma-Aldrich, Cat #HPA045511), anti-EMRE (Bethyl Laboratories, Cat #A300-BL19208), anti-GRP75 (Santa Cruz, Cat #sc-133,137), anti-TOM20 (Cell Signaling Technology, Cat #42406), anti-AFG3L2 (Thermo Fisher Scientific, Cat #PA5–95347), anti-CLPB (ProteinTech, Cat #15743–1-AP), and anti-TMBIM5 (ProteinTech, Cat #16296–1-AP). All primary antibodies were diluted 1:1000.

4.4. Measurements of mitochondrial membrane potential

HeLa cells were loaded with 20 nM tetramethyl rhodamine methyl ester (TMRM) (Thermo Fisher Scientific, Cat #I34361) for 30 min at 37 °C, then transferred to the imaging system. The probe was excited at 560 nm, and emission was recorded in the 590–650 nm range. Image acquisition occurred every 10 s with a fixed exposure time of 100 msec. After 6 acquisitions, 10 μM carboxyl cyanide *p*-trifluoromethoxyphenylhydrazone (CCCP), an uncoupler of oxidative phosphorylation, was added to completely collapse the mitochondrial membrane potential (ΔΨ). TMRM imaging was performed on an inverted microscope (Zeiss Axiovert 200) with a 40×/1.3 N.A. PlanFluor objective. Excitation was provided by a Deltaram V high-speed monochromator (Photon Technology International) and a 75 W Xenon Arc lamp. Images were captured using an Evolve 512 Delta EMCCD (Photometrics) and the system was controlled by MetaMorph 7.5 (Molecular Devices), with the setup assembled by Crisel Instruments. Data are presented as the average background-corrected fluorescence under resting conditions and analyzed using the Fiji distribution of ImageJ.

4.5. Aequorin [Ca^{2+}] measurements

HeLa cells were seeded at 60 % confluence in a 24-well plate. The cells were then transfected with the cytosolic (cytAEQ) or low-affinity mitochondrial (mtAEQmut) aequorin probes, along with the indicated siRNA/esiRNA or plasmid, using a standard Ca^{2+}-phosphate transfection method, as already performed [40]. Ca^{2+} measurements were conducted using a PerkinElmer EnVision plate reader with a two-

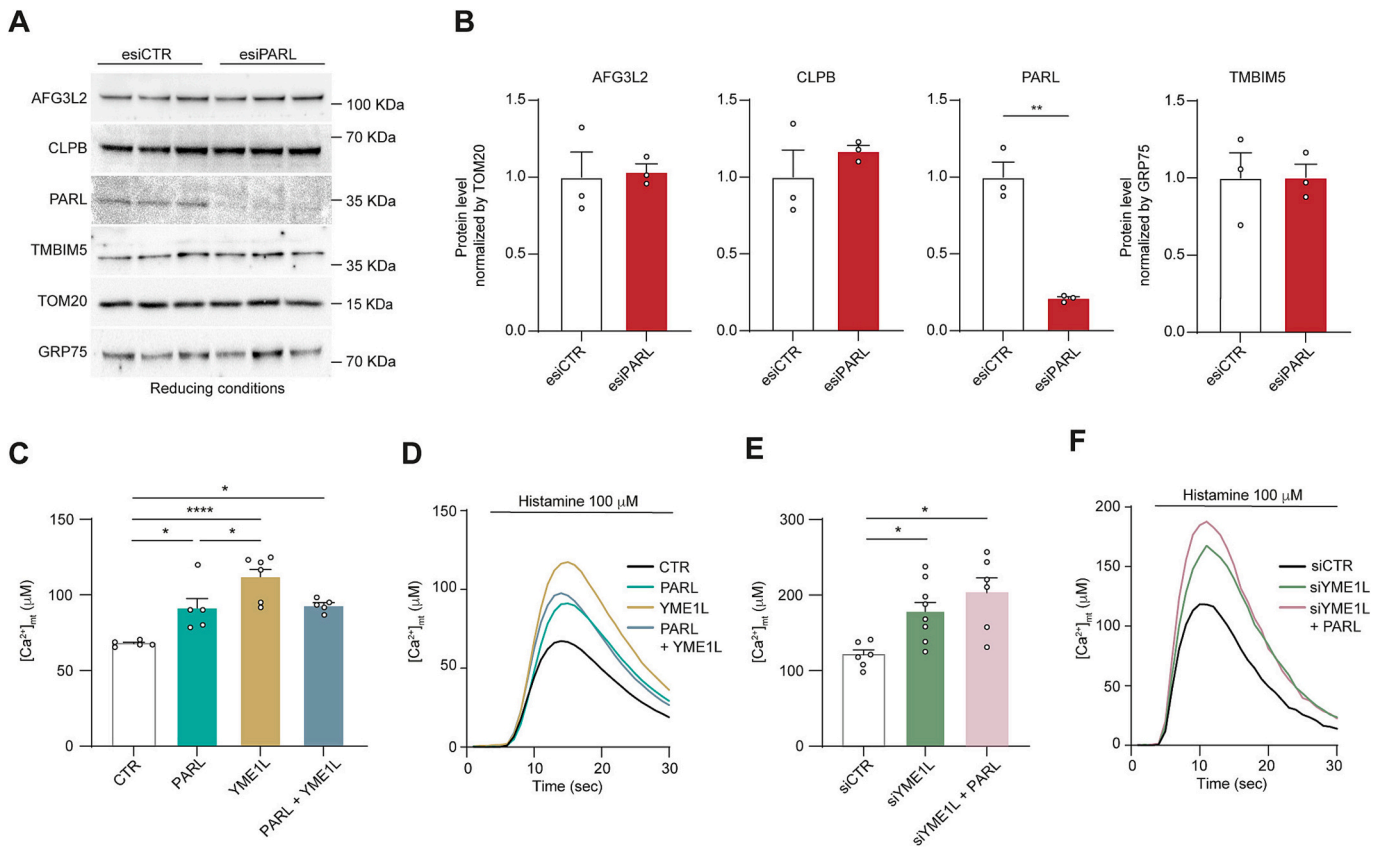

Fig. 7. PARL silencing does not affect the protein levels of AFG3L2, CLPB and TMBIM5, while the increase in mitochondrial Ca^{2+} uptake due to PARL overexpression is YME1L-interconnected. (A) Representative western blot of AFG3L2, CLPB, TMBIM5 and PARL obtained from the total protein extract of control (esiCTR) and PARL silenced (esiPARL) HeLa cells harvested 72 h after transfection. GRP75 or TOM20 were used as the loading control. n = 3. (B) Quantification of the western blot shown in A. (C) $[Ca^{2+}]_{mt}$ in intact HeLa cells overexpressing PARL, YME1L, or PARL together with YME1L for 48 h together with mitochondrially targeted aequorin, challenged with maximal histamine stimulation. The bar diagram represents the mean peak ± SEM. $n = 5$ for CTR, PARL and PARL + YME1L, n = 6 for YME1L. * $p \leq 0.05$, **** $p \leq 0.0001$ compared to the control (CTR). (D) Representative traces of the experiment performed in C. (E) $[Ca^{2+}]_{mt}$ in intact HeLa cells silencing YME1L alone or with the concomitant overexpression of PARL for 48 h together with mitochondrially targeted aequorin, challenged with maximal histamine stimulation. The bar diagram represents the mean peak ± SEM. n = 6 for siCTR and siYME1L + PARL, $n = 8$ for siYME1L. * $p \leq 0.05$ compared to the control (CTR). (F) Representative traces of the experiment performed in E.

injector unit. Briefly, cells were transfected in 24-well plates and then transferred to a 96-well plate (1:5 dilution) the day before the experiment. One hour before measurement, the apo-aequorin was reconstituted by incubating cells with 5 μM coelenterazine in 70 l of modified KRB buffer. Luminescence was measured for 1 min in each well. To induce Ca^{2+} transients, 100 μM histamine was injected, followed by 100 μM digitonin in a hypotonic Ca^{2+}-rich medium to discharge the remaining aequorin pool. Data were analyzed and calibrated using a custom-made Excel workbook. The mitochondrial and cytosolic Ca^{2+} influx rates were calculated as the maximal influx speed divided by the peak $[Ca^{2+}]$ after histamine stimulation, while the mitochondrial and cytosolic Ca^{2+} efflux rates were calculated as the maximal efflux speed divided by the peak $[Ca^{2+}]$ after histamine stimulation.

4.6. Co-IP experiment

For the interaction analysis between PARL-Flag and MICU1-HA, MICU2-HA, Hela cells were transfected with the indicated constructs using a standard Ca^{2+}-phosphate transfection method [40]. After 48 h, cells were lysed in Co-IP buffer (50 mM HEPES, 150 mM NaCl, 5 mM EDTA, 0.5 % DDM) supplemented with Complete EDTA-free Protease Inhibitor cocktail (Roche, Cat #11836170001), and Phosphatases Inhibitor cocktail (Roche, Cat #4906837001). Lysates were centrifuged at 15000*g* for 10 min at 4 °C, and the supernatants were collected. 1 mg of protein was incubated overnight with monoclonal α-Flag-agarose-conjugated antibody (Millipore, Cat #A2220) under rotation, following the manufacturer's instructions for co-immunoprecipitation. The next day, the agarose beads were washed three times with lysis buffer, and the immune complexes were eluted by heating at 95 °C for 5 min in NuPAGE LDS Sample Buffer (Thermo Fisher Scientific, Cat #NP0007). Both whole cell lysates (Input) and immunoprecipitated samples (IP: Flag) were subjected to Western blotting. Co-immunoprecipitated proteins were detected using anti-Flag (Cell Signaling Technology, Cat #2368) to visualize overexpressed PARL-Flag, anti-HA (Cell Signaling Technology, Cat #3734) to visualize overexpressed MICU1-HA and MICU2-HA, and anti-YME1L (Sigma-Aldrich, Cat #SAB1301252) to visualize endogenous YME1L. The primary antibodies were diluted 1:1000.

4.7. Statistical analysis of data

GraphPad Prism software was used to analyze the statistical significance of all data. The data are presented as mean ± SEM. Depending on the experiments, a Student's *t*-test, Mann-Whitney t-test, and one-way ANOVA were applied. $p \leq 0.05$ was considered significant.

CRediT authorship contribution statement

Donato D'Angelo: Writing – original draft, Validation, Investigation. **Aya Al Saidi:** Writing – original draft, Visualization, Investigation.

Giorgia Ghirardo: Writing – original draft, Validation, Investigation. **Denis Vecellio Reane:** Investigation. **Nicola Gasparini:** Investigation. **Rosario Rizzuto:** Writing – review & editing, Writing – original draft, Conceptualization. **Anna Raffaello:** Writing – review & editing, Writing – original draft, Conceptualization.

Declaration of competing interest

The authors declare that they have no known competing financial interests or personal relationships that could have appeared to influence the work reported in this paper.

Acknowledgments

The graphical abstract was created with BioRender, which we acknowledge. This research was supported with funding from the Italian Ministry of Health (RF-2016-02363566 to R.R.), the Italian Ministry of University and Research (PRIN 2020R2BP2E_002 to R.R., PRIN 20207P85MH to A.R.), the CARIPARO foundation (to R.R.), and the National Center for Gene Therapy and Drugs Based on RNA Technology, funded in the framework of the National Recovery and Resilience Plan (NRRP), Mission 4, Component 2, Investment 1.4, funded by the European Union - Next Generation EU, Project CN00000041, CUP C93C22002780006, Spoke n. 4 "Metabolic and Cardiovascular diseases" to R.R.

Appendix A. Supplementary data

Supplementary data to this article can be found online at https://doi.org/10.1016/j.bbamcr.2025.119998.

Data availability

Data will be made available on request.

References

[1] H.M. Ni, J.A. Williams, W.X. Ding, Mitochondrial dynamics and mitochondrial quality control, Redox Biol. 4 (2015) 6–13, https://doi.org/10.1016/j.redox.2014.11.006.
[2] J. Song, J.M. Herrmann, T. Becker, Quality control of the mitochondrial proteome, Nat. Rev. Mol. Cell Biol. 22 (2021) 54–70, https://doi.org/10.1038/s41580-020-00300-2.
[3] M.J. Baker, T. Tatsuta, T. Langer, Quality control of mitochondrial proteostasis, Cold Spring Harb. Perspect. Biol. 3 (2011), https://doi.org/10.1101/cshperspect.a007559.
[4] P.M. Quiros, T. Langer, C. Lopez-Otin, New roles for mitochondrial proteases in health, ageing and disease, Nat. Rev. Mol. Cell Biol. 16 (2015) 345–359, https://doi.org/10.1038/nrm3984.
[5] S. Deshwal, K.U. Fiedler, T. Langer, Mitochondrial proteases: multifaceted regulators of mitochondrial plasticity, Annu. Rev. Biochem. 89 (2020) 501–528, https://doi.org/10.1146/annurev-biochem-062917-012739.
[6] L. Lysyk, R. Brassard, E. Arutyunova, V. Siebert, Z. Jiang, E. Takyi, M. Morrison, H. S. Young, M.K. Lemberg, A.J. O'Donoghue, M.J. Lemieux, Insights into the catalytic properties of the mitochondrial rhomboid protease PARL, J. Biol. Chem. 296 (2021) 100383, https://doi.org/10.1016/j.jbc.2021.100383.
[7] L. Lysyk, R. Brassard, N. Touret, M.J. Lemieux, PARL protease: a glimpse at intramembrane proteolysis in the inner mitochondrial membrane, J. Mol. Biol. 432 (2020) 5052–5062, https://doi.org/10.1016/j.jmb.2020.04.006.
[8] M. Spinazzi, B. De Strooper, PARL: the mitochondrial rhomboid protease, Semin. Cell Dev. Biol. 60 (2016) 19–28, https://doi.org/10.1016/j.semcdb.2016.07.034.
[9] T. Wai, S. Saita, H. Nolte, S. Muller, T. Konig, R. Richter-Dennerlein, H.G. Sprenger, J. Madrenas, M. Muhlmeister, U. Brandt, M. Kruger, T. Langer, The membrane scaffold SLP2 anchors a proteolytic hub in mitochondria containing PARL and the i-AAA protease YME1L, EMBO Rep. 17 (2016) 1844–1856, https://doi.org/10.15252/embr.201642698.
[10] K. Walder, L. Kerr-Bayles, A. Civitarese, J. Jowett, J. Curran, K. Elliott, J. Trevaskis, N. Bishara, P. Zimmet, L. Mandarino, E. Ravussin, J. Blangero, A. Kissebah, G. R. Collier, The mitochondrial rhomboid protease PSARL is a new candidate gene for type 2 diabetes, Diabetologia 48 (2005) 459–468, https://doi.org/10.1007/s00125-005-1675-9.
[11] A.E. Civitarese, P.S. MacLean, S. Carling, L. Kerr-Bayles, R.P. McMillan, A. Pierce, T.C. Becker, C. Moro, J. Finlayson, N. Lefort, C.B. Newgard, L. Mandarino, W. Cefalu, K. Walder, G.R. Collier, M.W. Hulver, S.R. Smith, E. Ravussin, Regulation of skeletal muscle oxidative capacity and insulin signaling by the mitochondrial rhomboid protease PARL, Cell Metab. 11 (2010) 412–426, https://doi.org/10.1016/j.cmet.2010.04.004.
[12] M. Hatunic, M. Stapleton, E. Hand, C. DeLong, V.E. Crowley, J.J. Nolan, The Leu262Val polymorphism of presenilin associated rhomboid like protein (PARL) is associated with earlier onset of type 2 diabetes and increased urinary microalbumin creatinine ratio in an Irish case-control population, Diabetes Res. Clin. Pract. 83 (2009) 316–319, https://doi.org/10.1016/j.diabres.2008.12.004.
[13] B.L. Powell, S. Wiltshire, G. Arscott, P.A. McCaskie, J. Hung, B.M. McQuillan, P. L. Thompson, K.W. Carter, L.J. Palmer, J.P. Beilby, Association of PARL rs3732581 genetic variant with insulin levels, metabolic syndrome and coronary artery disease, Hum. Genet. 124 (2008) 263–270, https://doi.org/10.1007/s00439-008-0552-2.
[14] G. Shi, J.R. Lee, D.A. Grimes, L. Racacho, D. Ye, H. Yang, O.A. Ross, M. Farrer, G. A. McQuibban, D.E. Bulman, Functional alteration of PARL contributes to mitochondrial dysregulation in Parkinson's disease, Hum. Mol. Genet. 20 (2011) 1966–1974, https://doi.org/10.1093/hmg/ddr077.
[15] E. Deas, H. Plun-Favreau, S. Gandhi, H. Desmond, S. Kjaer, S.H. Loh, A.E. Renton, R.J. Harvey, A.J. Whitworth, L.M. Martins, A.Y. Abramov, N.W. Wood, PINK1 cleavage at position A103 by the mitochondrial protease PARL, Hum. Mol. Genet. 20 (2011) 867–879, https://doi.org/10.1093/hmg/ddq526.
[16] C. Meissner, H. Lorenz, A. Weihofen, D.J. Selkoe, M.K. Lemberg, The mitochondrial intramembrane protease PARL cleaves human Pink1 to regulate Pink1 trafficking, J. Neurochem. 117 (2011) 856–867, https://doi.org/10.1111/j.1471-4159.2011.07253.x.
[17] C. Meissner, H. Lorenz, B. Hehn, M.K. Lemberg, Intramembrane protease PARL defines a negative regulator of PINK1- and PARK2/Parkin-dependent mitophagy, Autophagy 11 (2015) 1484–1498, https://doi.org/10.1080/15548627.2015.1063763.
[18] K. Yamano, R.J. Youle, PINK1 is degraded through the N-end rule pathway, Autophagy 9 (2013) 1758–1769, https://doi.org/10.4161/auto.24633.
[19] S.M. Jin, M. Lazarou, C. Wang, L.A. Kane, D.P. Narendra, R.J. Youle, Mitochondrial membrane potential regulates PINK1 import and proteolytic destabilization by PARL, J. Cell Biol. 191 (2010) 933–942, https://doi.org/10.1083/jcb.201008084.
[20] D. Narendra, A. Tanaka, D.F. Suen, R.J. Youle, Parkin is recruited selectively to impaired mitochondria and promotes their autophagy, J. Cell Biol. 183 (2008) 795–803, https://doi.org/10.1083/jcb.200809125.
[21] S. Sekine, Y. Kanamaru, M. Koike, A. Nishihara, M. Okada, H. Kinoshita, M. Kamiyama, J. Maruyama, Y. Uchiyama, N. Ishihara, K. Takeda, H. Ichijo, Rhomboid protease PARL mediates the mitochondrial membrane potential loss-induced cleavage of PGAM5, J. Biol. Chem. 287 (2012) 34635–34645, https://doi.org/10.1074/jbc.M112.357509.
[22] N. Ishihara, K. Mihara, PARL paves the way to apoptosis, Nat. Cell Biol. 19 (2017) 263–265, https://doi.org/10.1038/ncb3504.
[23] S. Saita, H. Nolte, K.U. Fiedler, H. Kashkar, A.S. Venne, R.P. Zahedi, M. Kruger, T. Langer, PARL mediates Smac proteolytic maturation in mitochondria to promote apoptosis, Nat. Cell Biol. 19 (2017) 318–328, https://doi.org/10.1038/ncb3488.
[24] S. Saita, T. Tatsuta, P.A. Lampe, T. Konig, Y. Ohba, T. Langer, PARL partitions the lipid transfer protein STARD7 between the cytosol and mitochondria, EMBO J. 37 (2018), https://doi.org/10.15252/embj.201797909.
[25] M. Spinazzi, E. Radaelli, K. Horre, A.M. Arranz, N.V. Gounko, P. Agostinis, T. M. Maia, F. Impens, V.A. Morais, G. Lopez-Lluch, L. Serneels, P. Navas, B. De Strooper, PARL deficiency in mouse causes Complex III defects, coenzyme Q depletion, and Leigh-like syndrome, Proc. Natl. Acad. Sci. U. S. A. 116 (2019) 277–286, https://doi.org/10.1073/pnas.1811938116.
[26] H. Delgado de la Herran, D. Vecellio Reane, Y. Cheng, M. Katona, F. Hosp, E. Greotti, J. Wettmarshausen, M. Patron, H. Mohr, N. Prudente de Mello, M. Chudenkova, M. Gorza, S. Walia, M.S. Feng, A. Leimpek, D. Mielenz, N. S. Pellegata, T. Langer, G. Hajnoczky, M. Mann, M. Murgia, F. Perocchi, Systematic mapping of mitochondrial calcium uniporter channel (MCUC)-mediated calcium signaling networks, EMBO J. (2024), https://doi.org/10.1038/s44318-024-00219-w.
[27] Y. Sancak, A.L. Markhard, T. Kitami, E. Kovacs-Bogdan, K.J. Kamer, N.D. Udeshi, S. A. Carr, D. Chaudhuri, D.E. Clapham, A.A. Li, S.E. Calvo, O. Goldberger, V. K. Mootha, EMRE is an essential component of the mitochondrial calcium uniporter complex, Science 342 (2013) 1379–1382, https://doi.org/10.1126/science.1242993.
[28] D. D'Angelo, D. Vecellio Reane, A. Raffaello, Neither too much nor too little: mitochondrial calcium concentration as a balance between physiological and pathological conditions, Front. Mol. Biosci. 10 (2023) 1336416, https://doi.org/10.3389/fmolb.2023.1336416.
[29] R.R. Cupo, J. Shorter, Skd3 (human ClpB) is a potent mitochondrial protein disaggregase that is inactivated by 3-methylglutaconic aciduria-linked mutations, Elife 9 (2020), https://doi.org/10.7554/eLife.55279.
[30] M.J. Baker, K.U. Blau, A.J. Anderson, C.S. Palmer, L.F. Fielden, J.J. Crameri, D. Milenkovic, D.R. Thorburn, A.E. Frazier, T. Langer, D. Stojanovski, CLPB disaggregase dysfunction impacts the functional integrity of the proteolytic SPY complex, J. Cell Biol. 223 (2024), https://doi.org/10.1083/jcb.202305087.
[31] M. Patron, V. Checchetto, A. Raffaello, E. Teardo, D. Vecellio Reane, M. Mantoan, V. Granatiero, I. Szabo, D. De Stefani, R. Rizzuto, MICU1 and MICU2 finely tune the mitochondrial Ca2+ uniporter by exerting opposite effects on MCU activity, Mol. Cell 53 (2014) 726–737, https://doi.org/10.1016/j.molcel.2014.01.013.
[33] T. MacVicar, Y. Ohba, H. Nolte, F.C. Mayer, T. Tatsuta, H.G. Sprenger, B. Lindner, Y. Zhao, J. Li, C. Bruns, M. Kruger, M. Habich, J. Riemer, R. Schwarzer, M. Pasparakis, S. Henschke, J.C. Bruning, N. Zamboni, T. Langer, Lipid signalling drives proteolytic rewiring of mitochondria by YME1L, Nature 575 (2019) 361–365, https://doi.org/10.1038/s41586-019-1738-6.

[34] L. Zhang, F. Dietsche, B. Seitaj, L. Rojas-Charry, N. Latchman, D. Tomar, R.C. Wust, A. Nickel, K.B. Frauenknecht, B. Schoser, S. Schumann, M.J. Schmeisser, J. Vom Berg, T. Buch, S. Finger, P. Wenzel, C. Maack, J.W. Elrod, J.B. Parys, G. Bultynck, A. Methner, TMBIM5 loss of function alters mitochondrial matrix ion homeostasis and causes a skeletal myopathy, Life Sci Alliance 5 (2022), https://doi.org/10.26508/lsa.202201478.

[35] S. Austin, R. Mekis, S.E.M. Mohammed, M. Scalise, W.A. Wang, M. Galluccio, C. Pfeiffer, T. Borovec, K. Parapatics, D. Vitko, N. Dinhopl, N. Demaurex, K. L. Bennett, C. Indiveri, K. Nowikovsky, TMBIM5 is the Ca(2+) /H(+) antiporter of mammalian mitochondria, EMBO Rep. 23 (2022) e54978, https://doi.org/10.15252/embr.202254978.

[36] M. Patron, D. Tarasenko, H. Nolte, L. Kroczek, M. Ghosh, Y. Ohba, Y. Lasarzewski, Z.A. Ahmadi, A. Cabrera-Orefice, A. Eyiama, T. Kellermann, E.I. Rugarli, U. Brandt, M. Meinecke, T. Langer, Regulation of mitochondrial proteostasis by the proton gradient, EMBO J. 41 (2022) e110476, https://doi.org/10.15252/embj.2021110476.

[37] D. D'Angelo, V.H. Sanchez-Vazquez, B. Cartes-Saavedra, D. Vecellio Reane, R. R. Cupo, H. Delgado de la Herran, G. Ghirardo, J. Shorter, R.A. Wevers, S. B. Wortmann, F. Perocchi, R. Rizzuto, A. Raffaello, G. Hajnoczky, Dependence of mitochondrial calcium signalling and dynamics on the disaggregase, CLPB, Nat. Commun. 16 (2025) 2810, https://doi.org/10.1038/s41467-025-57641-9.

[38] C. Petrungaro, K.M. Zimmermann, V. Kuttner, M. Fischer, J. Dengjel, I. Bogeski, J. Riemer, The Ca(2+)-dependent release of the Mia40-induced MICU1-MICU2 Dimer from MCU regulates mitochondrial Ca(2+) uptake, Cell Metab. 22 (2015) 721–733, https://doi.org/10.1016/j.cmet.2015.08.019.

[39] T. Konig, S.E. Troder, K. Bakka, A. Korwitz, R. Richter-Dennerlein, P.A. Lampe, M. Patron, M. Muhlmeister, S. Guerrero-Castillo, U. Brandt, T. Decker, I. Lauria, A. Paggio, R. Rizzuto, E.I. Rugarli, D. De Stefani, T. Langer, The m-AAA protease associated with neurodegeneration limits MCU activity in mitochondria, Mol. Cell 64 (2016) 148–162, https://doi.org/10.1016/j.molcel.2016.08.020.

[40] A. Tosatto, R. Rizzuto, C. Mammucari, Ca(2+) measurements in mammalian cells with aequorin-based probes, Bio-Protoc. 7 (2017), https://doi.org/10.21769/BioProtoc.2155.